Manufacturing Science and Education 2025

ACTA TECHNICA NAPOCENSIS

Series: Applied Mathematics, Mechanics, and Engineering
Vol. 68, Issue Special II, Month July, 2025

EFFECT OF PROCESS PARAMETERS ON THE COMPRESSIVE BEHAVIOR OF PEKK PARTS FABRICATED BY MATERIAL EXTRUSION ADDITIVE MANUFACTURING

Paul Sebastian SUCIU, Sebastian - Marian ZAHARIA, Lucia – Antoneta CHICOS, Mihai Alin POP, Camil LANCEA

Abstract: *The material polyetherketoneketone (PEKK), belongs to the high-performance polymers family and has exceptional mechanical strength, thermal stability and chemical resistance. The material is used in the process of fused filament fabrication (FFF) and have been used in many applications for medical sector, automotive and aerospace. The scope of this study was to analyze the influence of the 3D printing parameters, the internal configuration type (honeycomb) and the infill density on the compressive strength of the 3D printed PEKK-SC specimens. Following the tests, it was concluded that the Fast Honeycomb pattern has higher compressive strength in comparation with the Full Honeycomb configuration. Infill density plays an important role when it comes to 3D printed products and the results related to this study suggests that the value of the compressive strength increases as the percentage of infill density goes up. The Shore D hardness of the material was determined and the microscopic analyze of FFF printed specimens was conducted as well.*
Keywords: *PEKK filament, compression tests, 3D printing, microscopic analysis, hardness Shore D.*

1. INTRODUCTION

Honeycomb configuration represents a structure similar to bee honeycomb, which has a hexagonal pattern, and have important applications related to the industry (aerospace, automotive, naval, constructions). Honeycomb configuration plays an important role when it comes to sandwich structures. It is one of the most important cellular cores. The honeycomb core can be manufactured from metallic materials, composites, aramids, plastics and presents the characteristics of low density, high rigidity, good stability, high energy absorption and high mechanical performances when compared with the foams [1, 2].

Honeycomb structures can be produced using classic procedures like expansion process and corrugated honeycomb manufacturing process [3, 4] or it can be produced using additive manufacturing [5, 6]. The additive manufacturing processes represents, in our days, one of the most common ways to obtain cellular structures, using materials like plastics, composites or even metals [7]. The additive manufacturing processes are diverse, fast and can use a wide range of materials (plastics, metals, ceramics, short fiber-reinforced composites, long fiber-reinforced composites, high strength polymers), from which can result a prototype or a fully functional product.

The honeycomb structure fabrication is well suited to the additive manufacturing process because the complex geometry models are made more cost-effective with a continuous improvement in the fabrication process in very short period of time due to the testing activities and topological optimizations of the model [8]. The honeycomb configuration was recognized as one of the strongest structures in terms of mechanical strength [7, 9] and thus, most of the software systems dedicated to additive manufacturing preparations implemented this type of internal configuration [10], among other types of patterns specific to the 3D printing procedures (grid, triangle, cubic, zigzag, cross 3D etc.). The major advantage of fused filament fabrication (FFF) is the capacity to produce

tridimensional cellular structures, with different internal configurations, in a short period of time whit the help of a digital model made beforehand [11].

The development of cellular structures is a point of interest for both research an industry, so the honeycomb structures were modified, optimized and FEA analyzed in order to obtain high mechanical performances while being lightweight [12]. In this context [13], four structures (honeycomb, square honeycomb, quasi-square honeycomb, and re-entrant honeycomb) were 3D printed and tested to compression, thus resulting that the wall thickness, 3D printing sequence, geometry and the Poisson ratio of the cell have a significant impact on the mechanical performances. Previous studies on internal configuration for 3D printed specimens that were flexural, and compression tested, suggests that the honeycomb configuration have similar or better performances for compression tests [14] and 3 points bending tests [15], compared to standard infill patterns.

Another important parameter for the FFF process is infill density which is defined as quantity of 3D printed filament inside the model and has direct impact on the structural performances, mass and the amount of time needed for the part to be 3D printed [16]. Reports from several studies indicates that a higher infill density corresponds to a higher tensile [17], compression [18] and 3 point bending strength [19] for the 3D printed parts. For industrial applications which require dimensional stability at high temperatures, good chemical resistance and high mechanical performances in comparation to standard filaments, and which needs a good mass/resistance ratio, high performance polymers are recommended, materials like PEI, PEEK, PEEK-CF, PEKK, TPI, PA, PPSU [20].

Because high performance polymers were developed recently, most of the studies, [21, 22, 23] focused on the defects analyses and the influence of 3D printing parameters on mechanical performances (tensile, compression, 3 points bending). The scope of this study was to analyze the influence of internal configuration (honeycomb) and infill density on the compression characteristics of the parts manufactured through fused filament fabrication process using the filament PEKK-SC (PolyEtherKetoneKetone).

2. MATERIALS AND METHODS

Taking in consideration the D695-15 standard [24], specific to plastic material testing, applied to the 3D printed parts, the specimens for plane strain compression tests analyzed in this study were designed using SolidWorks 2022 software system. The cylindrical specimens tested for flatwise compression have the following characteristics: diameter 12.7 mm and a height of 25.4 mm (Figure 1).

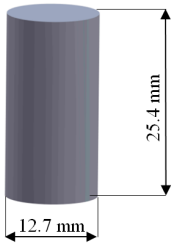

Fig. 1. The CAD model of the compression tested specimen.

In this study, the compression tested specimens, with honeycomb configuration, were produced using the FFF process with the MiniFactory Ultra 3D printing system, using Kimya PEKK-SC filament (Figure 2).

Fig. 2. The compression specimens manufactured with MiniFactory Ultra system.

The PEKK-SC filament [25] is a semi-crystalline thermoplastic polymer which has: heigh temperature resistance (up to 260 °C), excellent mechanical properties, certified for the aerospace domain FAR 25.853. The properties and the mechanical performances of PEKK-SC filament [25], were presented in Table 1 and Table 2.

Table 1

PEKK-SC filament properties [25].

Properties	Test methods	Values
Diameter	INS-6712	1.75 mm
Density	ISO 1183-1	1.27 g/cm^3
Moisture rate	INS-6711	< 1 %
Heat distortion temperature (HDT) (1.8 MPa)	ISO 75f	172°C
Glass Transition temperature (Tg)	ISO 11357-1 DSC (10°C/min - 20-410 °C)	161 °C
Melting Temperature (Tm)	ISO 11357-1 DSC (10 °C/min – 20-410 °C)	332 °C

Table 2

The mechanical properties of the 3D printed parts from PEKK-SC filament [25].

Properties	Test methods	XZ direction	ZX direction
Tensile strength	ISO 527	64.1 MPa	32.4 MPa
Tensile modulus	ISO 527	2.448 GPa	2.784 GPa
Flexural strength	ISO 178	79.3 MPa	61.6 MPa
Flexural modulus	ISO 178	1.918 GPa	1.705 GPa
Charpy impact resistance	ISO 179	5.35 kJ/m²	1.9 kJ/m²

The manufacturing parameters of the compression specimens, produced with FFF process, was presented Tabel 3.

Table 3

The manufacturing parameters of the FFF process for the compression-tested specimens made from PEKK-SC filament.

FFF parameters	Value
Layer height	0.25 mm
Top/ Bottom solid layers	5
Outline perimeters	3
Infill density	25%, 50%, 75%, 100%
Internal infill pattern	Full Honeycomb, Fast Honeycomb
Extrusion temperature	375°C
Heated bed	160°C
Heated chamber	150°C
Printing speed	50 mm/sec

The preparation for the 3D printing process of the specimens was carried out using the Simplify3D 5.1.1 software. To determine the compressive performance of the 3D-printed parts, made from PEKK-SC, the infill configuration (Full Honeycomb and Fast Honeycomb) and the infill density (25%, 50%, 75%, 100%) were varied.

Using Simplify3D software, the parts were manufactured in three steps: in the first step (Figure 3), parts with the Full Honeycomb infill pattern were printed at three different infill densities (25%, 50%, 75%); in the second step (Figure 4), parts with the Fast Honeycomb infill pattern were printed at the same three infill densities (25%, 50%, 75%); and in the final step, the parts with 100% infill density were produced.

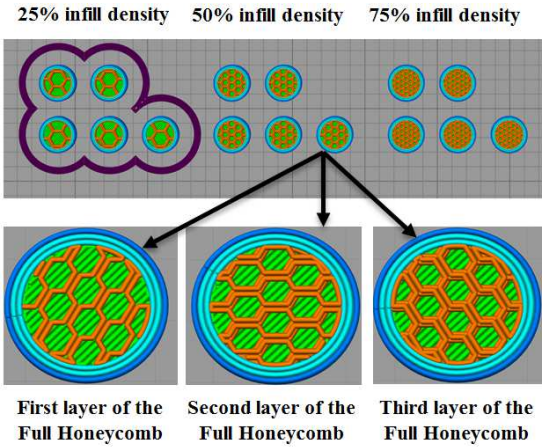

Fig. 3. The 3D printed parts with the Full Honeycomb configuration at different infill densities.

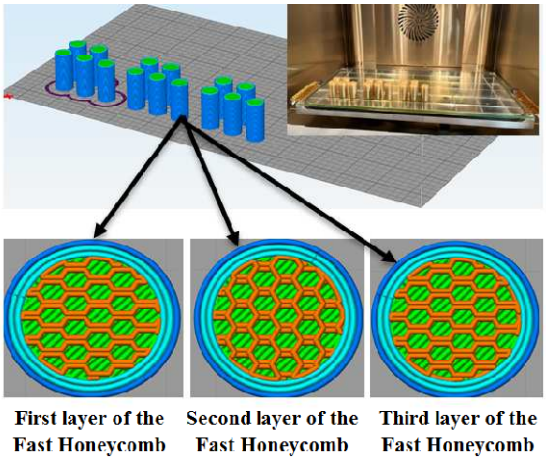

Fig. 4. The 3D printed parts with the Fast Honeycomb configuration at different infill densities.

The compression testes of the specimens were carried out using the WDW-150S testing machine, with a crosshead speed of 10 mm/min (Figure 5). For the compression tests, five specimens were manufactured for each of the two internal configurations (Full Honeycomb and Fast Honeycomb) at three infill densities (25%, 50%, 75%), resulting in a total of 30 specimens. Additionally, the last type of 3D printed specimens was produced with a 100% infill density.

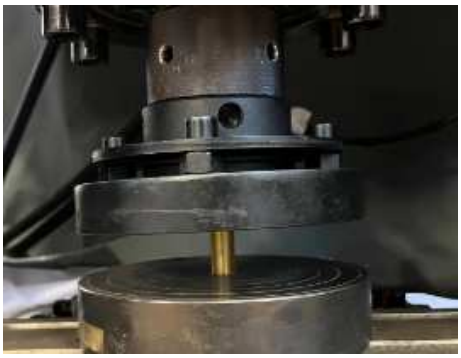

Fig. 5. Compression test for the specimen manufactured using the FFF process.

To determine the hardness, seven measurements were performed for each specimen using the Shore D durometer (Figure 6). The hardness value was determined in seven points following the path described in Figure 7.

Fig. 6. The Shore D durometer used for the hardness testing of the 3D printed parts.

For microscopic analysis and hardness tests (Figure 7), the specimens were cut in a vertical section (parallel to the build direction) and a horizontal section (perpendicular to the build direction).

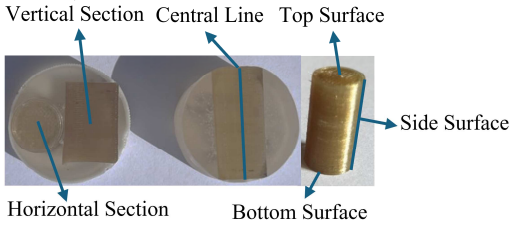

Fig. 7. The sectioning method of 3D printed parts for microscopic analysis and hardness determination.

The 3D printed samples were embedded in epoxy resin and polished with abrasive paper (Figure 7) of progressively finer grit size (600, 1200, 1500, 2000, and 2500) using the Buehler Phoenix Beta Grinder equipment (Figure 8). Finally, they were polished on alumina felt.

Fig. 8. The sample preparation equipment for the analysis of 3D printed parts.

The microscopic analysis of the 3D printed parts was performed using the Leica Emspira 3 optical microscope (Figure 9).

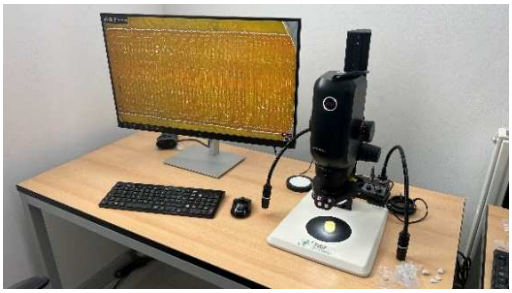

Fig. 9. The optical microscope used for the microscopic analysis of 3D printed parts.

3. RESULTS AND DISCUSSIONS

3.1 The compression tests of 3D printed specimens

Compression tests are used to determine the compressive performance: compressive strength, compressive modulus of elasticity, and Stress-Strain curves of 3D printed PEKK-SC parts.

In this study, five specimens with a honeycomb pattern (Fast Honeycomb - hereafter referred to as H-Fast-Infill density, and Full Honeycomb - hereafter referred to as H-Full-Infill density), manufactured thru FFF process, were flatwise compression tested. Using the WDW-150S testing machine and its integrated software system, the Stress-Strain curves and the mechanical properties (compressive strength and compressive modulus of elasticity) of the 3D printed PEKK-SC parts were determined (Figure 10).

The compressive mechanical performances of the 3D printed parts were analyzed from two perspectives: infill density (varying from 25%, 50%, 75%, to 100%) and infill configuration (Full Honeycomb and Fast Honeycomb). For the 3D printed PEKK-SC specimens, the mean values of compressive strength and compressive modulus of elasticity were determined based on the performed tests (5 at number). From Figure 10, it can be observed that, in terms of internal configuration, the compression test results indicates that the Fast Honeycomb structure exhibits higher performance by a boundary of 2% to 4% (for the 75% infill density) compared to the Full Honeycomb structure.

This difference between the two internal configurations can primarily be attributed to the higher density of the hexagon-type topologies in the Fast Honeycomb configuration. In addition, the second contributing factor is the layer deposition pattern, which ensures a better coverage of the entire infill area of the cylindrical specimens (Figure 4).

For the Full Honeycomb pattern, the average compressive strength values range from 49 MPa (Full Honeycomb - 25% infill density) to 68.3 MPa (Full Honeycomb - 75% infill density). For the Fast Honeycomb configuration, the compressive strength varies between 49.8 MPa (Fast Honeycomb - 25% infill density) and 71.5 MPa (Fast Honeycomb - 75% infill density). The average value of the modulus of elasticity for both internal configurations maintained approximately the same differences as those observed in compressive strength.

Analyzing the results in terms of infill density, it can be stated that infill density significantly influences the compressive behavior of parts manufactured using the FFF process. The specimens manufactured using the FFF process with the lowest infill density (25%) failed under the lowest applied load (approximately 6 kN), consequently exhibiting the lowest compressive strength of 49 MPa (Figure 10).

Doubling the infill density to 50% led to a 25% increase in compressive strength for specimens with both internal configurations. Increasing the infill density to 75% resulted in a 44% higher compressive strength compared to the specimens with a 25% infill density and a 15% increase compared to those with a 50% infill density. As was expected, the 3D printed PEKK-SC specimens with 100% infill density withstand the highest compressive force (13.5 kN), exhibiting a maximum compressive strength of 109 MPa.

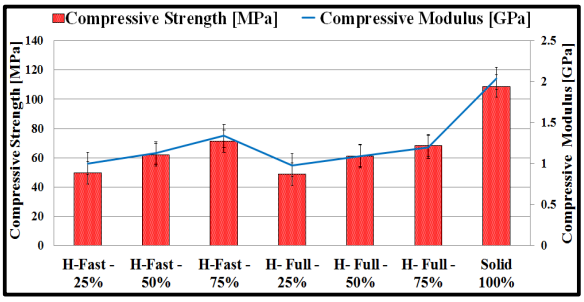

Fig. 10. The results of the compression tests for 3D printed PEKK-SC parts.

The compressive strength of specimens with 100% infill density is 118% higher compared to those with 25% infill density, a fact that has been highlighted in other studies as well [26, 27]. However, the 3D printing with 100% infill density also has disadvantages [28, 29]: high consumption of extruded material, increased costs of printed parts, especially when using high-performance polymer filaments, longer manufacturing time, and increased part weight.

The behavior of the specimens, in terms of the Stress-Strain relationship (Figure 11), for the Full Honeycomb pattern (with three different infill densities) and the 100% infill density

specimens tested for compression, indicates a linear Stress-Strain relationship followed by a decrease in compressive strength at the failure point of the 3D printed parts.

The plastic deformation of the 3D printed specimens with a 25% infill density was the longest, whereas the specimens with a 100% infill density exhibited the shortest plastic deformation. Lower-density parts deform more easily under compressive loads, while higher-density parts are more resistant [30,31] and exhibit lower deformations (Figure 11).

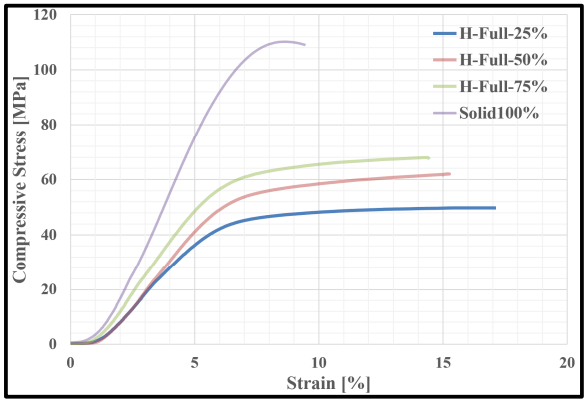

Fig. 11. Stress-Strain curves for 3D printed parts with the Full Honeycomb configuration at different infill densities.

For the 3D printed specimens with the Fast Honeycomb configuration, the elastic deformation interval was identified, where stress increased with strain. In the plastic deformation stage, after reaching the maximum compressive strength, stress either decreased or fluctuated slightly as strain increased (Figure 12).

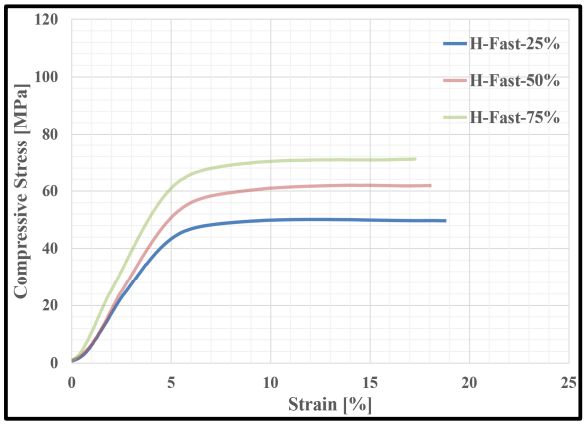

Fig. 12. Stress–Strain curves for 3D printed parts with the Fast Honeycomb configuration at different infill densities.

The main statistical indicators of the specimens manufactured using the FFF process from PEKK-SC filament were determined for the 35 specimens tested for compression.

Table 4

Statistical indicators determined from the compression tests of 3D printed parts – compressive strength [MPa].

Specimen type	Mean	Standard deviation	Coefficient of variation
H-Fast-25% - Compressive Strength [MPa]	49.8	1.1	2.2
H-Fast - 50% - Compressive Strength [MPa]	62.3	1.5	2.4
H-Fast - 75% - Compressive Strength [MPa]	71.5	1.5	2.1
H- Full - 25%- Compressive Strength [MPa]	49	1.22	2.5
H- Full - 50% - Compressive Strength [MPa]	61.5	1.14	1.85
H- Full - 75% - Compressive Strength [MPa]	68.3	1.14	1.67
Solid 100% - Compressive Strength [MPa]	109	1.58	1.45

The statistical indicators (mean, standard deviation, and the coefficient of variation) were determined for the 3D printed PEKK-SC parts manufactured using the FFF process. These indicators were calculated for the two internal configurations (Full Honeycomb and Fast Honeycomb) and the four infill density types (25%, 50%, 75%, 100%), following the statistical relationships outlined in the D695-15 standard for each data series (compressive strength and compressive modulus).

In the analysis of compressive strength, when the coefficient of variation (CV) is close to zero (CV < 30%), the data obtained from compression testing (the coefficient of variation value ranges between 1.67% and 2.5%) are considered homogeneous and the calculated mean is representative [32] for these datasets (Table 4). The coefficient of variation provides a clear indication of the homogeneity of the

obtained data from the compression tests of 3D printed parts.

As shown in Table 5, the coefficient of variation [33] ranges from 0.67% to 2.82% (compressive modulus of elasticity). Therefore, it can be concluded that the mean values are representative of all seven data sets obtained from the compression tests.

Table 5

Statistical indicators determined from the compression tests of 3D printed parts - compressive modulus of elasticity [GPa].

Specimen type	Mean	Standard deviation	Coefficient of variation
H-Fast - 25% - Compressive Modulus [GPa]	0.99	0.02	2.08
H-Fast - 50%- Compressive Modulus [GPa]	1.13	0.02	1.98
H-Fast - 75% - Compressive Modulus [GPa]	1.33	0.01	0.67
H- Full - 25% - Compressive Modulus [GPa]	0.98	0.03	2.82
H- Full - 50% - Compressive Modulus [GPa]	1.09	0.02	1.59
H- Full - 75%- Compressive Modulus [GPa]	1.23	0.02	1.78
Solid 100% - Compressive Modulus [GPa]	2.04	0.03	1.23

3.2 The hardness tests of 3D printed parts

Shore hardness is used to evaluate the hardness of various materials, serving as a critical factor in determining if a material is suitable for practical applications, recently studied for 3D printed materials as well [34, 35]. For the hardness test of 3D-printed parts, four surfaces were examined according to Figure 7 (top surface, bottom surface, side surface, central line). Using a durometer, seven measurements were performed on each of the four surfaces of 3D printed parts with 100% infill density, and the average Shore hardness values were presented in Figure 13. The measurements revealed that the central line exhibited the highest hardness value (86.1 D), while the hardness values varied between the upper and lower surfaces of the 3D-printed parts (Figure 13). A possible explanation for the higher hardness on the lower surface could be attributed to the repeated heating cycles of the extruded layers, as well as the constant build platform temperature (160 °C), to which the lower region was exposed during the FFF process.

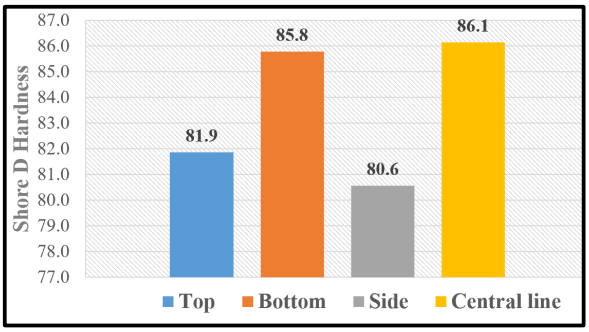

Fig. 13. Hardness measurements of 3D printed parts.

3.3 Microscopic analysis of 3D printed parts

For the compression tested specimens, similar failure patterns were identified, exhibiting local buckling of the outer walls, along with densification of the extruded material layers, which contributes to the barreling effect of the parts.

The barreling effect causes deformation of the tested specimen (Figure 14) under an axial compressive force and is associated with the phenomenon of local buckling.

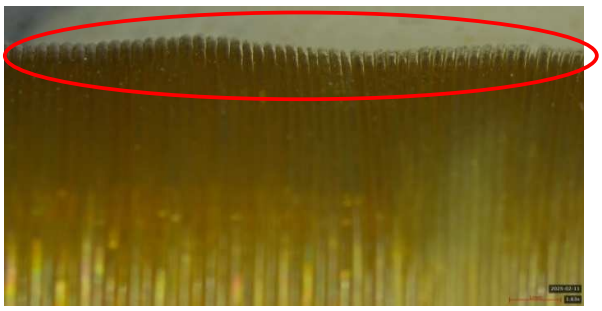

Fig. 14. Local buckling of outer surfaces after compression tests.

Regarding the vertical section (Figure 15), typical 3D printing defects [36], such as triangular voids, were observed, especially in the three outer walls of the parts. In the horizontal section (Figure 16), the three walls and a homogeneous infill with minimal defects can be seen in the 3D printed PEKK-SC parts.

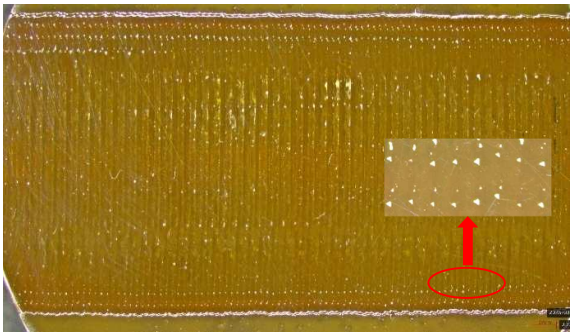

Fig. 15. Triangular voids in the Vertical Section of 3D Printed Parts.

Fig. 16. Horizontal Section of 3D Printed Parts.

4. CONCLUSION

The fused filament fabrication (FFF) process enables the production of adjacent hexagonal cells at low costs, in a short period of time by utilizing the infill density parameter. The analysis conducted in this study leads to the following conclusions:

- The Fast Honeycomb internal configuration exhibited 2%-4% higher compressive strength compared to the Full Honeycomb configuration;
- Compressive strength increases proportionally with the infill density of 3D printed parts;
- The mean compressive strength of a 3D printed part made from PEKK-SC filament with 100% infill density was 109 MPa;
- The mean maximum Shore D hardness for specimens with 100% infill density was 86.1;
- The hardness showed higher values in the lower part of the part, closer to the 3D printing platform;
- The specimens exhibited common 3D printing defects, such as triangular voids and gaps between extruded layers of material.

5. REFERENCES

[1] Rubio, E.M., Blanco, D., Marín, M.M., Carou, D., *Analysis of the latest trends in hybrid components of lightweight materials for structural uses*, Procedia Manufacturing, ISSN: 1877-7058, 2019

[2] Silva, R.D.C., Castro, G.M.D., Oliveira, A.B.D.S., Brasil, A.C.D.M., *Effect of 3D-Printed Honeycomb Core on Compressive Property of Hybrid Energy Absorbers: Experimental Testing and Optimization Analysis*, Materials, ISSN: 1996–1944, 2024

[3] Kress, G., Winkler. M., *Honeycomb sandwich residual stress deformation pattern*, Composite Structures, ISSN: 0263-8223, 2009

[4] Tripathi, L., Behera, B. K., *3D Woven honeycomb composites*, Journal of Materials Science, ISSN: 1573-4803, 2021

[5] Zaharia, S.M., Lancea, C., Chicos, L.A., Pop, M.A., Caputo, G., Serra, E., *Mechanical properties and corrosion behaviour of 316L stainless steel honeycomb cellular cores manufactured by selective laser melting*, Transactions of FAMENA, ISSN: 1333-1124, 2017

[6] Bates, S.R., Farrow, I.R., Trask, R.S., *Compressive behaviour of 3D printed thermoplastic polyurethane honeycombs with graded densities*, Materials & Design, ISSN: 1873-4197, 2019

[7] Kladovasilakis, N., Tsongas, K., Karalekas, D., Tzetzis, D., *Architected Materials for Additive Manufacturing: A Comprehensive Review*, Materials, ISSN: 1996-1944, 2022

[8] Palaniyappan, S., Sivakumar, N. K., Sikder, P., Alodhayb, A., Muthuramamoorthy, M., *Topological design factor optimization in the development of periodic-type honeycomb lattice structure on the carbon fiber reinforced polyethylene terephthalate glycol composite,* Polymer Composites, ISSN: 0272-8397, 2023

[9] Qi, C., Jiang, F., Yang, S., *Advanced honeycomb designs for improving mechanical properties: A review*, Composites Part B: Engineering, ISSN: 1359-8368, 2021

[10] Cabreira, V., Santana, R.M.C., *Effect of infill pattern in Fused Filament Fabrication*

(FFF) 3D Printing on materials performance, Matéria (Rio de Janeiro), ISSN: 1517-7076, 2020

[11] Ciobanu, R., Ciobanu, O., Malcoci, I. *Modern approach for design and manufacturing of products using FDM process*, Acta Technica Napocensis-Series: Applied Mathematics, Mechanics, and Engineering, ISSN: 1221 – 5872, 2024

[12] Kucewicz, M., Baranowski, P., Małachowski, J., *A method of failure modeling for 3D printed cellular structures*, *Materials & Design*, ISSN: 1873-4197, 2019

[13] Yang, D., Guo, L., Fan, C., *Mechanical Behavior of 3D-Printed Thickness Gradient Honeycomb Structures*, Materials, ISSN: 1996–1944, 2024

[14] León-Calero, M., Reyburn Valés, S. C., Marcos-Fernández, Á., Rodríguez-Hernandez, J., *3D printing of thermoplastic elastomers: Role of the chemical composition and printing parameters in the production of parts with controlled energy absorption and damping capacity*, Polymers, ISSN: 2073-4360, 2021

[15] Lopes, L., Reis, D., Paula Junior, A., Almeida, M., *Influence of 3D microstructure pattern and infill density on the mechanical and thermal properties of PET-G filaments*, Polymers, ISSN: 2073-4360, 2023

[16] Do, T. D., Le, M. C., Nguyen, T. A., Le, T. H., *Effect of infill density and printing patterns on compressive strength of ABS, PLA, PLA-CF materials for FDM 3D printing*, Materials Science Forum, ISSN: 1662-9752, 2022

[17] Chicos, L.A., Pop, M.A., Zaharia, S.M., Lancea, C., Buican, G.R., Pascariu, I.S., Stamate, V.M., *Fused Filament Fabrication of Short Glass Fiber-Reinforced Polylactic Acid Composites: Infill Density Influence on Mechanical and Thermal Properties*, Polymers, ISSN: 2073-4360, 2022

[18] Karad, A. S., Sonawwanay, P. D., Naik, M., Thakur, D. G. *Experimental study of effect of infill density on tensile and flexural strength of 3D printed parts*, Journal of Engineering and Applied Science, ISSN: 1110-1903, 2023

[19] Aloyaydi, B. A., Sivasankaran, S., Ammar, H.R., *Influence of infill density on microstructure and flexural behavior of 3D printed PLA thermoplastic parts processed by fusion deposition modeling*, AIMS Materials Science, ISSN: 2372-0484, 2019

[20] Junaid, M., uz Zaman, U. K., Naseem, A., Ahmad, Y., Aqeel, A. B. *Material selection in additive manufacturing for aerospace applications using multi-criteria decision making*, MATEC Web of Conferences, Vol. 398, pp. 01012, 2024

[21] Pulipaka, A., Gide, K.M., Beheshti, A., Bagheri, Z.S., *Effect of 3D printing process parameters on surface and mechanical properties of FFF-printed PEEK*, Journal of Manufacturing Processes, ISSN: 1526-6125, 2023

[22] Rashed, K., Kafi, A., Simons, R., Bateman, S., *Effects of fused filament fabrication process parameters on tensile properties of polyether ketone ketone (PEKK)*, The International Journal of Advanced Manufacturing Technology, ISSN: 0268-3768, 2022

[23] Paszkiewicz, S., Lesiak, P., Walkowiak, K., Irska, I., Miądlicki, K., Królikowski, M., Piesowicz, E. and Figiel, P., *The mechanical, thermal, and biological properties of materials intended for dental implants: a comparison of three types of poly (aryl-ether-ketones)(PEEK and PEKK)*, Polymers, ISSN: 2073-4360, 2023

[24] ASTM D695, Standard Test Method for Compressive Properties of Rigid Plastics, ASTM Materials Standards, PA, USA, 2002

[25] Kimya PEKK-SC 3D Filament, https://www.crea3d.com/en/kimya/880-1056-kimya-pekk-sc.html

[26] Vázquez-Silva, E., Pintado-Pintado, J. A., Moncayo-Matute, F. P., Torres-Jara, P. B., Moya-Loaiza, D. P., *Effect of Infill Density on the Mechanical Properties of Natural PEEK Processed by Additive Manufacturing*, *Polymers*, ISSN: 2073-4360, 2025

[27] Challa, B. T., Gummadi, S. K., Elhattab, K., Ahlstrom, J., Sikder, P., *In-house processing of 3D printable polyetheretherketone (PEEK) filaments and the effect of fused deposition modeling parameters on 3D-printed PEEK*

structures, The International Journal of Advanced Manufacturing Technology, ISSN: 0268-3768, 2022
[28] Hasan, M. R., Davies, I. J., Pramanik, A., John, M., Biswas, W. K., *Potential of recycled PLA in 3D printing: A review,* Sustainable manufacturing and service economics, ISSN: 2667-3444, 2024
[29] Dos Reis, M. Q., Carbas, R. J., Marques, E. A., da Silva, L. F., *Effect of the Infill Density on 3D-Printed Geometrically Graded Impact Attenuators, Polymers*, ISSN: 2073-4360, 2024
[30] Mazlan, M.A., Anas, M.A., Nor Izmin, N.A., Abdullah, A.H., *Effects of infill density, wall perimeter and layer height in fabricating 3D printing products*, Materials, ISSN: 1996–1944, 2023
[31] Liu, J., Naeem, M.A., Al Kouzbary, M., Al Kouzbary, H., Shasmin, H.N., Arifin, N., Abd Razak, N.A., Abu Osman, N.A., *Effect of infill parameters on the compressive strength of 3D-printed nylon-based material*, Polymers, ISSN: 2073-4360, 2023
[32] Grimaldo Ruiz, O., Rodriguez Reinoso, M., Ingrassia, E., Vecchio, F., Maniero, F., Burgio, V., Civera, M., Bitan, I., Lacidogna, G., Surace, C., *Design and mechanical characterization using digital image correlation of soft tissue-mimicking polymers*, Polymers, ISSN: 2073-4360, 2022
[33] Zaharia, S.M., Enescu, L.A., Pop, M.A., *Mechanical performances of lightweight sandwich structures produced by material extrusion-based additive manufacturing*, *Polymers*, ISSN: 2073-4360, 2020.
[34] Ansari, A. A., Kamil, M., *Izod impact and hardness properties of 3D printed lightweight CF-reinforced PLA composites using design of experiment*, International Journal of Lightweight Materials and Manufacture, ISSN: 2589-7225, 2022
[35] Wang, Z., Chen, X., Chen, X., Liang, J., Zeng, D., Gan, Y., *Effect of moisture content in polyether-ether-ketone (PEEK) filament on 3D printed parts*, Discover Applied Sciences, ISSN: 3004-9261, 2024
[36] Serino, G., Distefano, F., Zanetti, E. M., Pascoletti, G., Epasto, G., *Multiscale Mechanical Characterization of Polyether-2-ketone (PEKK) for Biomedical Application*, Bioengineering, ISSN: 2306-5354, 2024

Efectul parametrilor de proces asupra comportamentului de compresiune al pieselor din PEKK realizate prin fabricație aditivă cu extrudare de material

Materialul Polietercetonecetona (PEKK), face parte din familia polimerilor de înaltă rezistență având performanțe mecanice, termice și chimice excepționale și este utilizat în procedeul de fabricație cu filament fuzibil (FFF), având aplicații avansate în domeniul aviației, auto și medical. În cadrul acestui studiu s-a analizat influența parametrilor de fabricație, configurația internă de tip honeycomb și densitatea de umplere, asupra performanțelor la compresiune a specimenelor printate 3D din filamentul PEKK. În urma testelor la compresiune s-a evidențiat că tipul de configurație internă Fast Honeycomb a prezentat proprietăți la compresiune superioare în comparație cu configurația Full Honeycomb. Densitate de umplere joacă un rol important în printarea 3D a produselor, iar rezultatele acestui studiu au indicat o creștere a rezistenței la compresiune odată cu creșterea densității de umplere. De asemenea, s-a determinat duritate Shore D și au fost analizate microscopic specimenelor fabricate prin procedeul FFF.

Paul Sebastian SUCIU, PhD Student, Eng., Transilvania University of Brașov, Department of Manufacturing engineering, B-dul Eroilor No.29, Brașov, Romania, paul.suciu@unitbv.ro
Sebastian-Marian ZAHARIA, PhD Professor, Transilvania University of Brașov, Department of Manufacturing engineering, B-dul Eroilor No.29, Brașov, Romania, zaharia_sebastian@unitbv.ro
Lucia-Antoneta CHICOS, Associate Professor, Transilvania University of Brașov, Department of Manufacturing engineering, B-dul Eroilor No.29, Brașov, Romania, l.chicos@unitbv.ro
Mihai Alin POP, Researcher II, Transilvania University of Brasov, Materials Science Department, B-dul Eroilor No.29, Brașov, Romania, mihai.pop@unitbv.ro
Camil LANCEA, PhD Professor, Transilvania University of Brașov, Department of Manufacturing engineering, B-dul Eroilor No.29, Brașov, Romania, camil@unitbv.ro